NUCLEAR THEORY, Vol. 36 (2017)
eds. M. Gaidarov, N. Minkov, Heron Press, Sofia

On Possible Shape Isomers in Pre-Actinide Nuclei

B. Nerlo-Pomorska[1], **K. Pomorski**[1], **J. Bartel**[2], **C. Schmitt**[3]

[1]UMCS, 20031 Lublin, Poland
[2]IPHC, 67000 Strasbourg, France
[3]GANIL, 14000 Caen,France

Abstract. Using the macroscopic-microscopic model with the macroscopic energy determined by the Lublin-Strasbourg-Drop and the microscopic shell and pairing corrections evaluated through the Yukawa-folded mean-field potential, a certain number of yet unknown super- and hyper-deformed shapes isomers in even-even Pt, Hg, Pb, Po, Rn, and Ra isotopes are predicted. Quadrupole moments were evaluated in the local minima of the potential-energy surfaces and turned out to be in good agreement with the experimental data, that, for the time being, are only available in the ground states.

1 Introduction

The very broad fission barriers that are found in the the whole nuclear chart somewhere beyond Platinum indicate that the inclusion of shell effects will have a good chance to produce local minima in the potential energy surface of these nuclei corresponding to super- and hyper-deformed shapes. Extended calculations for long isotopic chains of even-even nuclei in that region have therefore been performed within the macroscopic-microscopic model. The Lublin-Strasbourg Drop (LSD) energy [1] has been used for the macroscopic part of the potential energy surface, while microscopic effects were evaluated in a Yukawa-folded single-particle potential [2] with the Strutinsky shell correction method [3] and the BCS [4] theory for pairing correlations. A new, Fourier expansion [5] of nuclear shapes developed by us is used to describe nuclear deformations. Several shape isomers could be identified in our calculations. Hope is that some of them can be found experimentally using e.g. proton beams that allow to produce compound systems with not too large angular momentum. Quadrupole moments of the most pronounced minima were evaluated.

2 Model

In order to describe shape isomeric states in general, and fission isomers in particular, one needs the energy of a given nucleus as a function of its deformation. Such a calculation relies on two essential ingredients. On one hand a description that is able to determine the energy of the studied nucleus as realistically as ever

possible. It is clear that the energy that one is speaking about needs to include the quantum-mechanical structure as well as the pairing correlations, and this for any nuclear deformation. Such a description could rely on some mean-field approach using nucleon-nucleon interaction rooted (more or less directly) in the meson fields or elementary nucleon-nucleon diffusion cross sections. Instead, and this is the method that is used in our present investigation, one could use the macroscopic-microscopic model to obtain this nuclear energy. On the other hand one also needs to describe the vast variety of nuclear shapes that are encountered in the course of the deformation process. In the case of the nuclear fission process, this is particularly demanding since very elongated and necked-in shapes have to be taken into account. As mentioned above, a new Fourier expansion [5] of nuclear shapes, presented in more detail below, is used in our calculation.

2.1 Fourier expansion of deformed shapes

The shape-profile function of a fissioning nucleus is expanded in a Fourier series:

$$\frac{\rho_s^2(z)}{R_0^2} = \sum_{n=1}^{\infty} \left[a_{2n} \cos\left(\frac{(2n-1)\pi}{2} \frac{z-z_{sh}}{z_0} \right) + a_{2n+1} \sin\left(\frac{2n\pi}{2} \frac{z-z_{sh}}{z_0} \right) \right], \quad (1)$$

where, in cylindrical coordinates, $\rho_s(z)$ is the distance of the nuclear surface perpendicular to the symmetry z-axis, and z_0 half the elongation of the nuclear shape along that axis. The shift coordinate z_{sh} ensures that the centre of mass of the nuclear shape can be located at the origin of the coordinate system. For the end points of the shape at $z_{sh} \pm z_0$ the condition $\rho_s(z) = 0$ is automatically satisfied by Eq. (1). One introduces an elongation parameter c through $z_0 = cR_0$, which is equal to unity for a sphere, smaller than one for oblate, and larger than one for prolate deformations. The parameters $a_2,\ a_3,\ a_4$ describe respectively quadrupole, octupole and hexadecapole deformations, or better to say, elongation, reflection asymmetry and neck degree of freedom. Since the path to fission now corresponds to decreasing values a_2 and growing negative values of a_4, we instead introduce new coordinates, having better suited and more intuitive properties for the discussion and further use of the potential-energy landscapes:

$$\begin{aligned} q_2 &= a_2^{(0)}/a_2 - a_2/a_2^{(0)}\,, \\ q_3 &= a_3\,, \\ q_4 &= a_4 + \sqrt{(q_2/9)^2 + (a_4^{(0)})^2} \end{aligned} \quad (2)$$

with $a_n^{(0)}$ being the value of the coordinate a_n for a spherical shape [5]. Non-axial shapes (η) can also be described in the present shape parametrization, but in none of the local minima in any of the investigated nuclei such a non-axiality was found to play any role. It is set to 0 in this contribution.

3 Deformation Energies

The calculation was carried out for even-even isotopes between Pt and Pu. Examples of the potential energy landscapes (relative to the spherical LSD energy) on q_2, q_3 plane (after minimization with respect to q_4) are shown in Figures 1-7 for Pt, Hg, Pb, Po, Rn and Ra even-even isotopes. Similar maps for Hg, Po and Ra have been published in Refs. [11,12], but we will repeat the conclusions concerning those nuclei in our present investigation. It appears interesting to follow the evolution (appearance and disappearance) of the different $superdeformed$, $hyperdeformed$, and $ultradeformed$ local minima.

Starting with the Pt isotopes shown in Figure 1, we observe two energy minima, one oblate and a deeper prolate. Beyond ^{186}Pt they become comparable in energy and tend towards the spherical shape which is reached at ^{192}Pt (N=114 which is a magic number).

In the Hg chain [11] shown in Figure 2 the static potential-energy suggests a fission partition that is reflection asymmetric, with a heavy-fragment mass of about 100-110 depending in the Hg isotope, in good agreement with the experiment [13]. It is important to emphasize that a clear evolution of the static fission path occurs with increasing Hg mass. Indeed, for the lightest $^{178-182}$Hg isotopes, an asymmetric valley appears already at $q_2 \approx 1$, while the minimum energy path evolves through a symmetric splitting for a sizeable part, and to an asymmetric partition only at the very last stage beyond $q_2 \approx 1.7$. This result corroborates previous conjectures [14].

The Pb isotopes displayed in Figures 3 and 4 exhibit a spherical ground state (magic Z=82 proton number favors a spherical shape in the ground state) for all isotopes, but the octupole energy minimum appears for ^{190}Pb. The superdeformed isomer arrives there up to ^{202}Pb, but the octupole one disappears. Then the ^{204}Pb - ^{208}Pb get the deep spherical ground state.

In the Po isotopic chain [11], [9] shown in Figure 5 the potential energy landscapes suggest a coexistence of symmetric and asymmetric fission for the most neutron deficient isotopes, whereas only symmetric fission is expected for the heavier isotopes. Such a prediction is in line with recent experimental data [15].

In the Rn isotopes even 4 octupole symmetric isomers can be observed in Figure 6 but above ^{208}Rn they slowly go towards a spherical, very deep in ^{210}Rn, minimum.

The survey of the Ra chain has shown in Figure 7 [11] that the path to fission corresponding to the minimum energy is reflection-symmetric for all light isotopes. An asymmetric valley progressively develops, however, with increasing Ra mass which competes with a symmetric splitting around ^{222}Ra, and finally becomes the favoured fission configuration for still heavier Ra. This evolution is again in good agreement with experimental data (see [16] and Refs. therein).

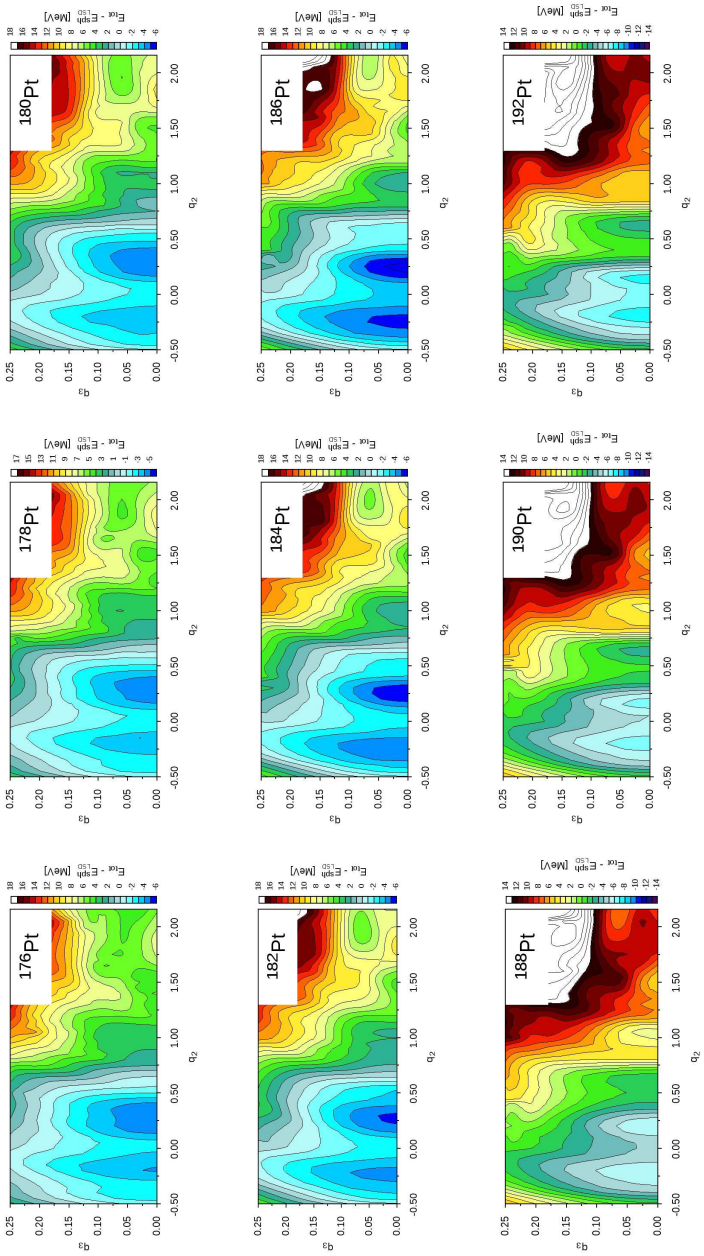

Figure 1. Potential energy landscapes (relative to the spherical LSD energy) on the (q_2, q_3) (elongation, octupole) plane for $\eta = 0$ and after minimisation with respect to the neck parameter q_4, of the Fourier expansion [5] for even-even Pt isotopes.

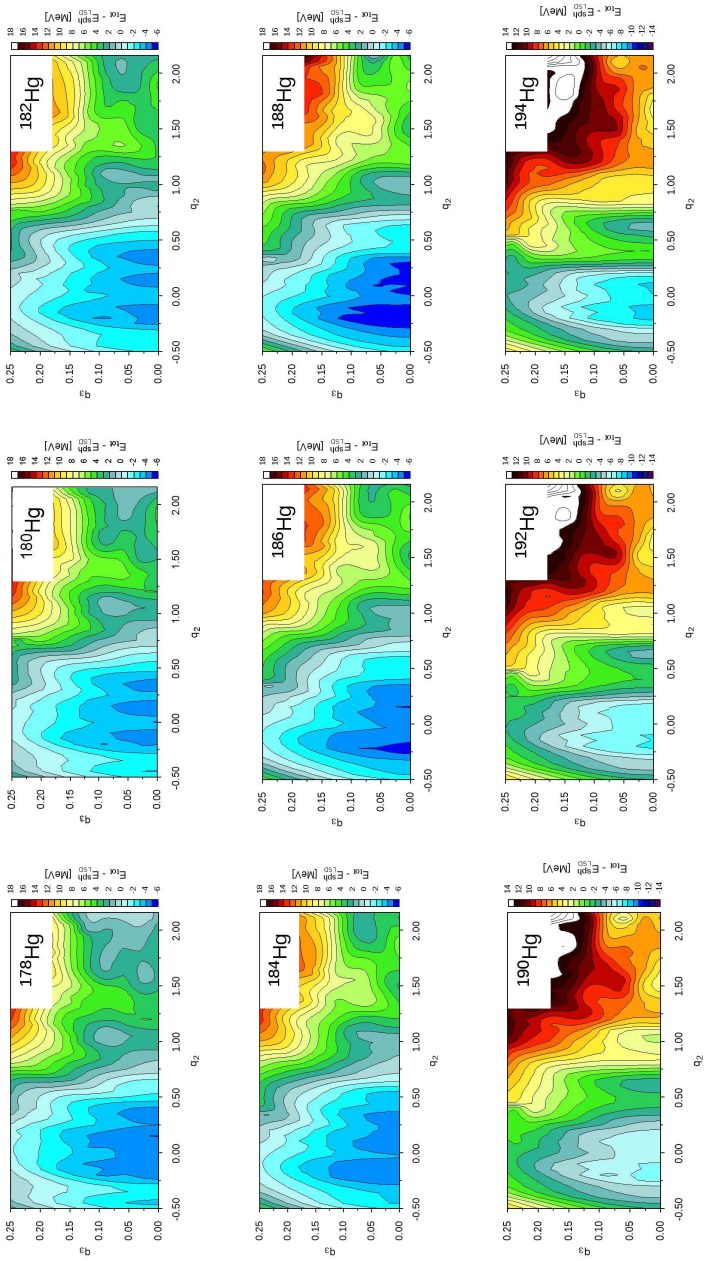

Figure 2. Potential energy landscapes (relative to the spherical LSD energy) on the (q_2, q_3) (elongation, octupole) plane for $\eta = 0$ and after minimisation with respect to the neck parameter q_4, of the Fourier expansion [5] for even-even Hg isotopes.

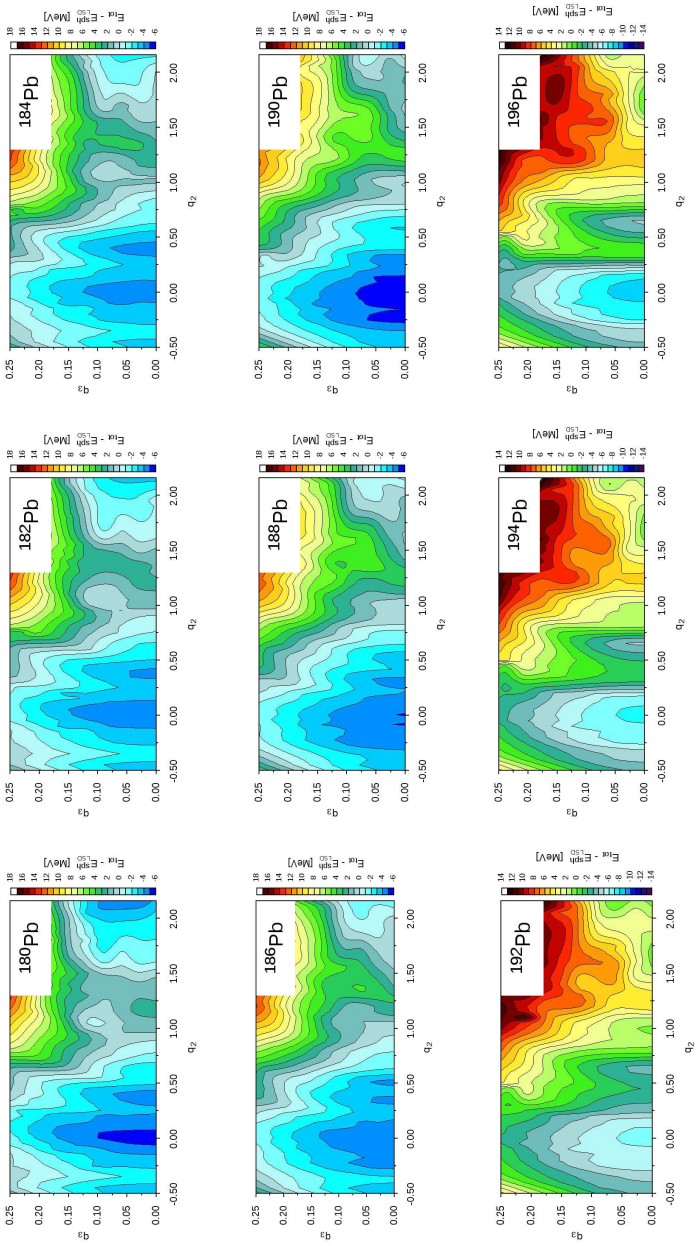

Figure 3. Potential energy landscapes (relative to the spherical LSD energy) on the (q_2, q_3) (elongation, octupole) plane for $\eta = 0$ and after minimisation with respect to the neck parameter q_4, of the Fourier expansion [5] for even-even ^{180}Pb to ^{196}Pb isotopes.

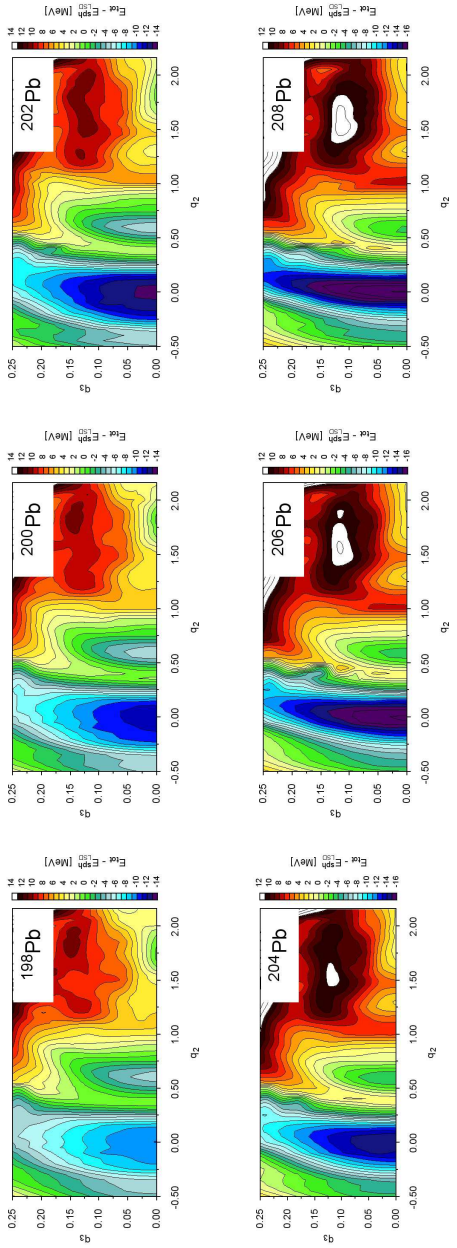

Figure 4. Potential energy landscapes (relative to the spherical LSD energy) on the (q_2, q_3) (elongation, octupole) plane for $\eta = 0$ and after minimisation with respect to the neck parameter q_4, of the Fourier expansion [5] for even-even ^{198}Pb to ^{208}Pb isotopes.

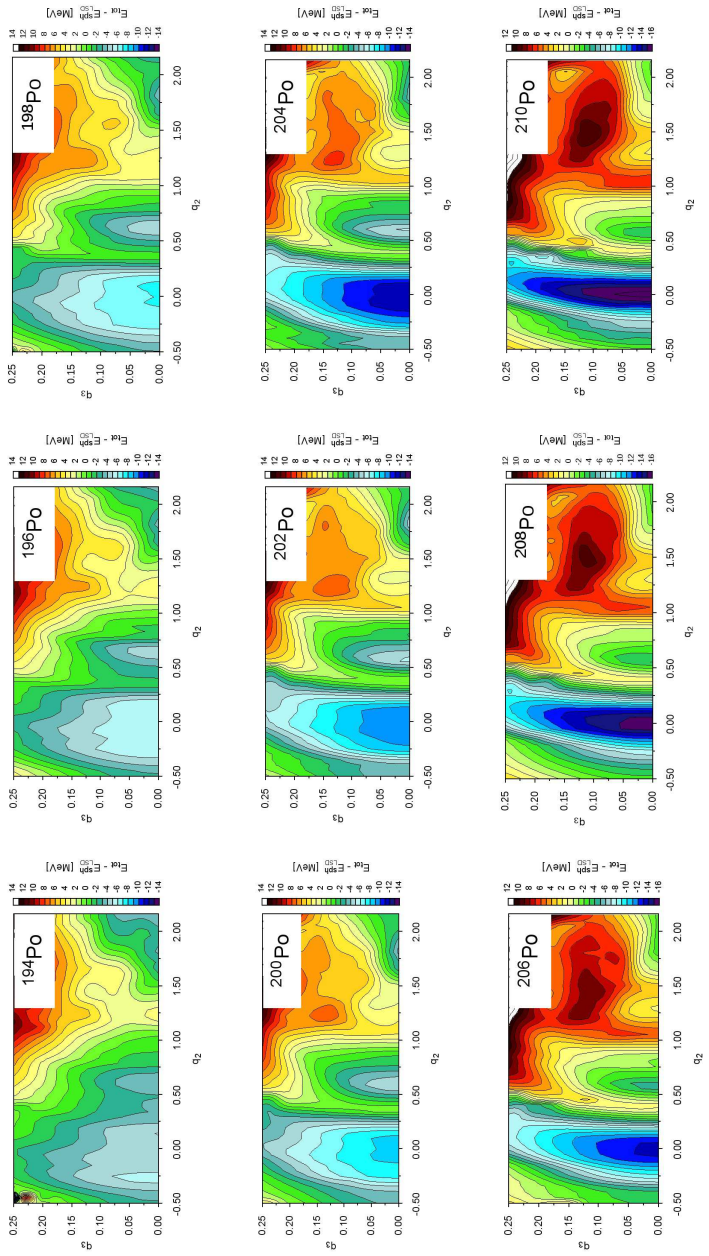

Figure 5. Potential energy landscapes (relative to the spherical LSD energy) on the (q_2, q_3) (elongation, octupole) plane for $\eta = 0$ and after minimisation with respect to the neck parameter q_4, of the Fourier expansion [5] for even-even Po isotopes.

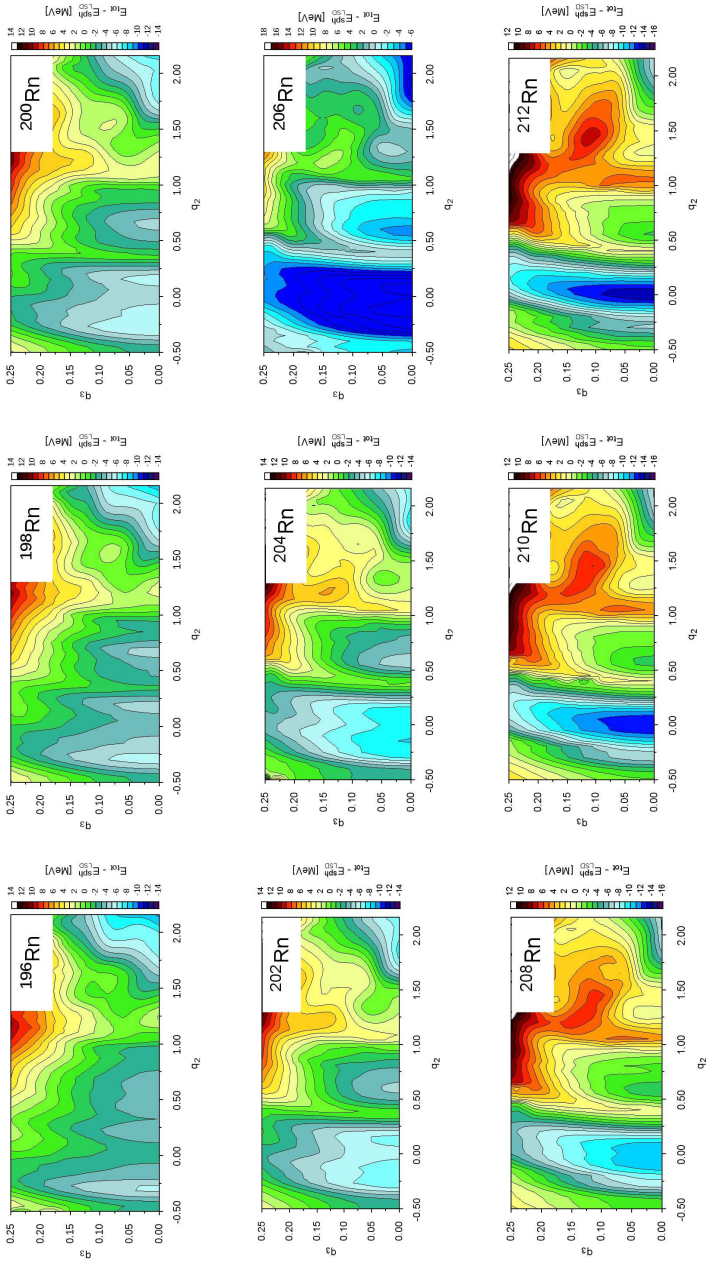

Figure 6. Potential energy landscapes (relative to the spherical LSD energy) on the (q_2, q_3) (elongation, octupole) plane for $\eta = 0$ and after minimisation with respect to the neck parameter q_4, of the Fourier expansion [5] for even-even Rn isotopes.

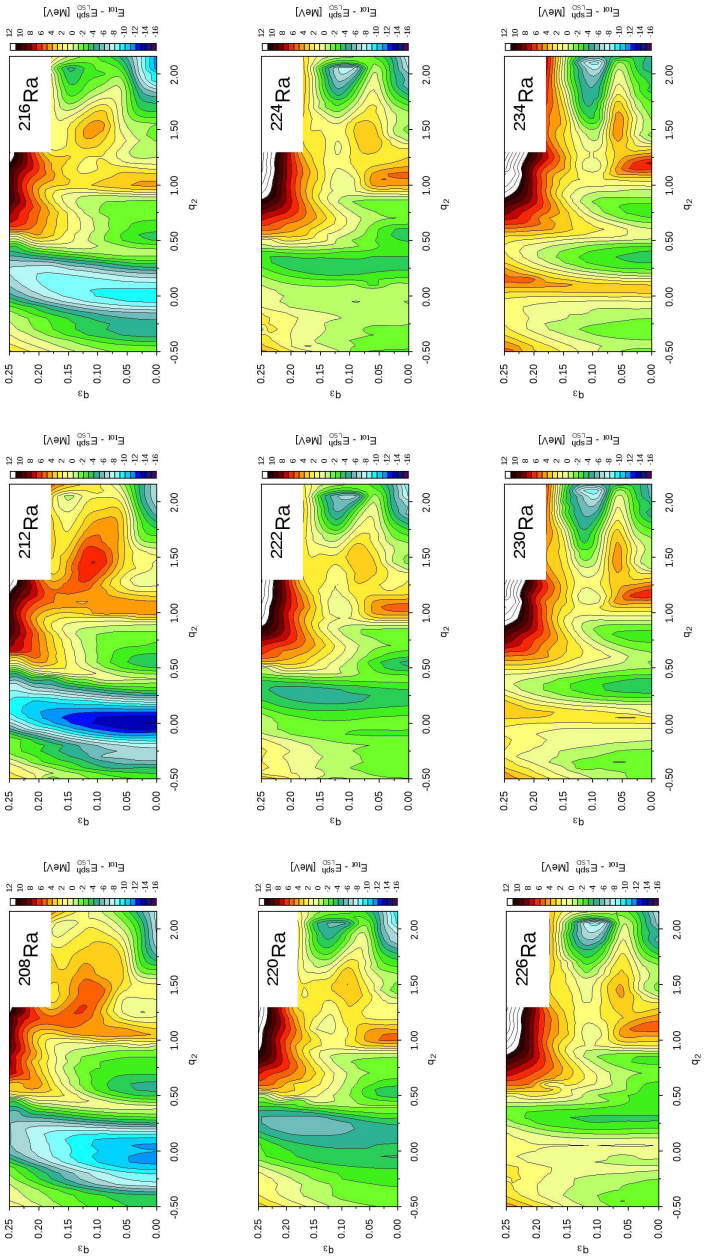

Figure 7. Potential energy landscapes (relative to the spherical LSD energy) on the (q_2, q_3) (elongation, octupole) plane for $\eta = 0$ and after minimisation with respect to the neck parameter q_4, of the Fourier expansion [5] for even-even Ra isotopes.

4 Electric Quadrupole Moments

The quadrupole moments associated with most pronounced energy minima were evaluated. The corresponding calculated electric quadrupole moments are presented in Figures 8 to 13 for the Pt–Ra isotopic chains in the shape isomers visible e.g. in the potential energy surfaces of Figures 1 to 7. They agree rather well with the available data for the ground state (gs), what allows to trust the model predictions. Experimental efforts to look for exotic shapes (super-deformed – sd, hyper-deformed – hd,hd1) in this region are strongly encouraged.

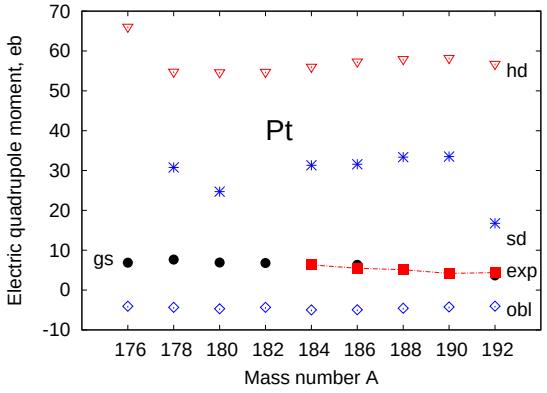

Figure 8. Electric quadrupole moments of even-even Pt isotopes for the ground states (gs), oblate(obl), super-deformed (sd) and hyper-deformed (hd) shape-isomers. The data (exp) for ground states are shown, where available [10].

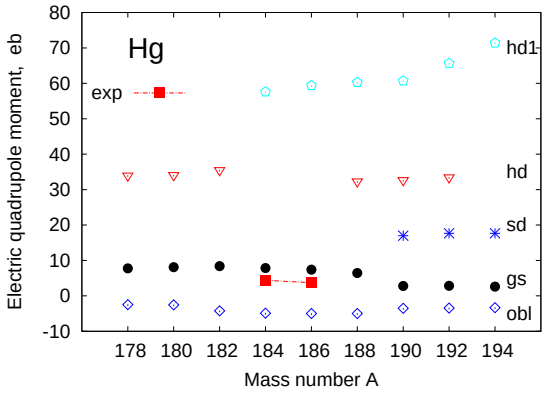

Figure 9. Electric quadrupole moments of even-even Hg isotopes for the ground states (gs), oblate(obl), super-deformed (sd) and hyper-deformed (hd,hd1) shape-isomers. The data (exp) for ground states are shown, where available [10].

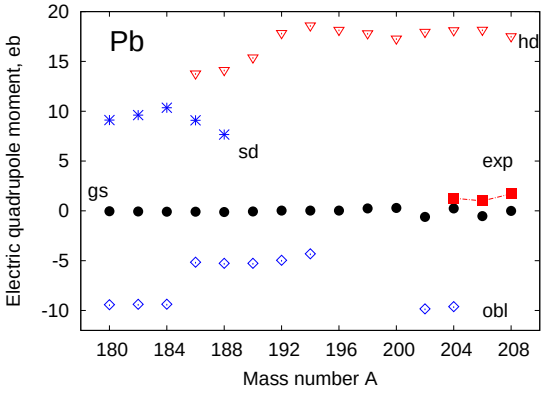

Figure 10. Electric quadrupole moments of even-even Pb isotopes for the ground states (gs), oblate(obl), super-deformed (sd) and hyper-deformed (hd) shape-isomers. The data (exp) for ground states are shown, where available [10].

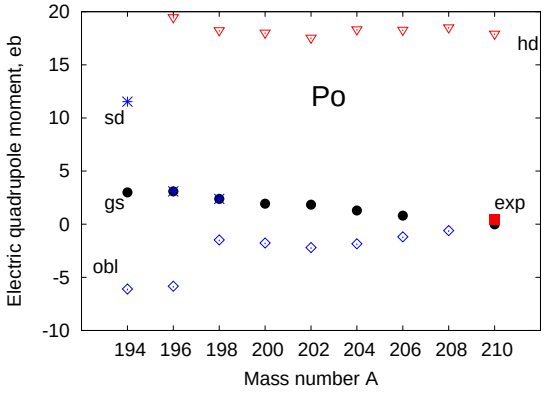

Figure 11. Electric quadrupole moments of even-even Po isotopes for the ground states (gs), oblate(obl), super-deformed (sd) and hyper-deformed (hd) shape-isomers. The data (exp) for ground states are shown, where available [10].

5 Summary

Our investigations of the liquid-drop fission barriers heights and their shapes performed in Ref. [17] in a variational calculation have shown that the fission barriers of medium-heavy nuclei are very broad and do not decrease rapidly when going from the saddle to the scission point. This property of the macroscopic energy offers a chance that in this region of nuclei shell effects may produce local minima corresponding to a large nuclear elongation. As first candidates, we have chosen the chains of Pt to Ra even-even [11] isotopes, and we have

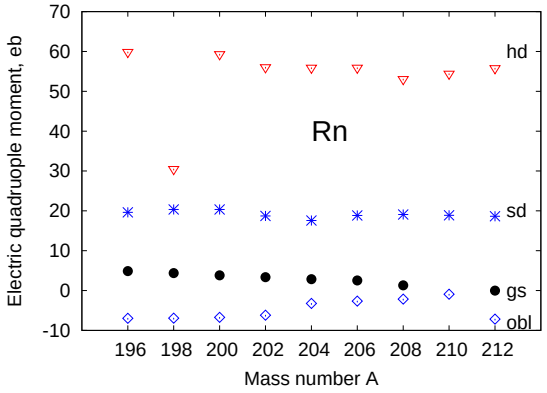

Figure 12. Electric quadrupole moments of even-even Rn isotopes for the ground states (gs), oblate(obl), super-deformed (sd) and hyper-deformed (hd) shape-isomers.

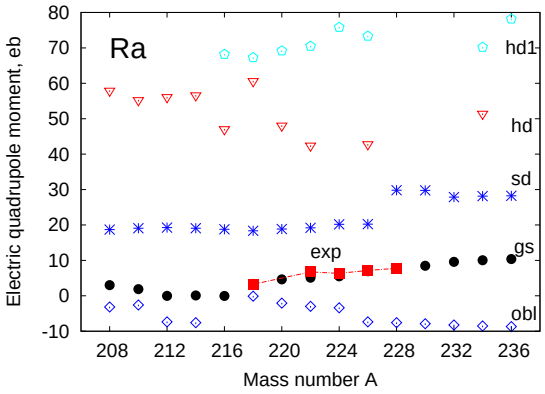

Figure 13. Electric quadrupole moments of even-even Ra isotopes for the ground states (gs), oblate(obl), super-deformed (sd) and hyper-deformed (hd,hd1) shape-isomers. The data (exp) for ground states are shown, where available [10].

shown that the microscopic energy corrections can, indeed, produce pronounced minima in the rather flat macroscopic potential-energy surfaces. The electric quadrupole moments for all the ground states and isomers were found and they reproduce rather well the data available for the ground state. In the case of very flat potential energy valleys the minima are not precise, so the agreement can be worse. The large $B(E2)$ transition probability corresponding to an electric quadrupole moment could be a fingerprint for such ultra-deformed isomers. We hope that in the near future this new island of super-, hyper- and ultra-deformed shape isomers will be discovered in the experimental analysis.

Acknowledgements

This work has been partly supported by the Polish-French COPIN-IN2P3 collaboration agreement under project number 08-131 and by the Polish National Science Centre, grant No. 2013/11/B/ST2/04087.

References

[1] K. Pomorski and J. Dudek, *Phys. Rev. C* **67** (2003) 044316.
[2] K.T.R. Davies and J.R. Nix, *Phys. Rev. C* **14** (1976) 1977.
[3] V.M. Strutinsky, *Nucl. Phys. A* **95** (1967) 420.
[4] S.G. Nilsson et al., *Nucl. Phys. A* **131** (1969) 1.
[5] K. Pomorski, B. Nerlo Pomorska, J. Bartel, C. Schmitt, *Acta. Phys. Polon* Supl. **8** (2015) 667.
[6] K. Pomorski and J. Bartel, *Int. J. Mod. Phys. E* **15** (2006) 417.
[7] J. Bartel, A. Dobrowolski, and K. Pomorski, *Int. J. Mod. Phys. E* **16** (2007) 459.
[8] J. Bartel, K. Pomorski, B. Nerlo-Pomorska, and C. Schmitt, *Phys. Scr.* **90** (2015) 114010.
[9] B. Nerlo Pomorska, K. Pomorski, J. Bartel, *Acta. Phys. Polon*. **B47** (2016) 943.
[10] http://www.nndc.bnl.gov/nudat2/.
[11] B. Nerlo Pomorska, K. Pomorski, J. Bartel, C. Schmitt, *Acta. Phys. Polon*. Supl. **10** (2017) 173.
[12] B. Nerlo Pomorska, K. Pomorski, J. Bartel, C. Schmitt, *Acta. Phys. Polon*. **B48** (2016) 451.
[13] A.N. Andreyev, et al., *Phys. Rev. Lett*. **105** (2010) 252502.
[14] T. Ichikawa, A. Iwamoto, P. Moller, and A.J. Sierk, *Phys. Rev. C* **86** (2012) 024610.
[15] L. Ghys et al., *Phys. Rev. C* **90** (2013) 041301(R).
[16] K.-H. Schmidt, et al., *Nucl. Phys. A* **665** (2000) 221.
[17] F. Ivanyuk and K. Pomorski, *Phys. Rev. C* **79** (2009) 054327.